Journal of Palaeosciences 72(2023): 81–89
2583-4266/2023
https://doi.org/10.54991/jop.2023.1849

Demonstration of process-based reconstruction of annual temperatures from tree ring oxygen isotope

TRINA BOSE[1] AND SUPRIYO CHAKRABORTY[2,3]

[1]Birbal Sahni Institute of Palaeosciences, 53 University Road, Lucknow 226 007, India.
Email: trinabose@bsip.res.in
[2]Indian Institute of Tropical Meteorology, Dr. Homi Bhabha Road, Pashan, Pune 411008, Maharashtra, India.
[3]Department of Atmospheric and Space Sciences, Savitribai Phule Pune University, Pune, Maharashtra, India.

(Received 14 January, 2023; revised version accepted 16 October, 2023)

ABSTRACT

Bose T & Chakraborty S 2023. Demonstration of process-based reconstruction of annual temperatures from tree ring oxygen isotope. Journal of Palaeosciences 72(2): 81–89.

Forecasting the global warming of the post-industrial period requires knowledge of natural variations in climatic parameters, especially temperature in preceding times. Due to its stable time resolution and known physiochemical formation process, tree ring cellulose isotope datasets have immense potential to yield climatic variability information. The first standardized site-independent temperature reconstruction model from tree-ring cellulose oxygen isotope data is demonstrated here using data from a montane site in the western Himalayas. This model does not require any statistical calibration and can be directly compared with instrumental or modelled data. The resulting temperature amplitude is dependent on moisture availability and this input is needed to modulate the reconstruction. The present work tests the possibility of input of carbon isotope discrimination as a proxy of relative humidity. This input achieved amplitude control but additional frequency components were introduced to the reconstruction.

Key-words—Tree ring, Oxygen isotope, Reconstruction, Temperature.

Terminology used

Terms:

‰ VPDB	per mil Vienna Pee Dee Belemnite
‰VSMOW	per mil Vienna Standard Mean Ocean Water
R_{SMOW}	Oxygen isotope ratio of SMOW = 0.0020052
R_{atm}	‰ VSMOW Oxygen isotope ($^{18}O/^{16}O$) ratio of atmospheric water vapour
δ_{ah}	$\delta^{18}O$ of atmospheric water vapour (‰ VSMOW)
δ_c	Tree ring cellulose $\delta^{18}O$ values (‰VSMOW)
δ_{sw}	Reconstructed oxygen isotope ($\delta^{18}O$) of soil water (‰VSMOW)
Δ_{cC}	Change in carbon isotopic composition from air CO_2 to tree ring cellulose
T_a	Air temperature (°C)
T_L	Leaf temperature (°C)
R_{hf}	Relative humidity, in fraction
P	Atmospheric Pressure (kPa)
e	Vapour Pressure (kPa)
C_s	Stomatal conductance ($mol m^{-2} s^{-1}$)

C_{bl} Boundary layer conductance ($molm^{-2}s^{-1}$)

Constants with respect to processes described in this article:

α_k Water liquid-vapour kinetic fractionation in air
= 1.0285 (Roden *et al*., 2000)
1.032 (Cappa *et al*., 2003)

α_{kb} Water liquid-vapour kinetic fractionation of boundary layer
= 1.0189 (Roden *et al*., 2000)
1.032 (Cappa *et al*., 2003)

f_O Fraction of oxygen isotopic exchange between cellulose and medium water
= 0.42

ε_{OA} fractionation for oxygen in autotrophic metabolism (sucrose) = 27

ε_{OH} fractionation for oxygen in heterotrophic metabolism (cellulose) = 27

Formulae:

R_{xy} Nx/Ny; where Nx and Ny are the abundances of heavier isotope (x) and lighter isotope (y) of a given element (e.g. ^{18}O and ^{16}O)

$\delta^{sample}_{standard}$ $\left(\frac{R_{sample} - R_{standard}}{R_{standard}}\right) \times 1000‰$

ΔT Difference between air temperature to that of the leaf (°C), $T_a - T_L$

α_L^* Water liquid-vapour equilibrium fractionation at leaf temperature
$= exp\ (\frac{1137}{(273.16 + T_L)^2} - \frac{0.4156}{273.16 + T_L} - 0.002066$ (Majoube, 1971)

INTRODUCTION

PROGRESSIVE anthropogenic climate change in the current times requires knowledge of natural variations in climatic parameters, especially temperature. The natural variation can only be seen in datasets that pre-date the industrial period (Steffen *et al*., 2016; Lewis & Maslin, 2015; Barnosky, 2014). The main climatic parameter reflecting anthropogenic change is the temperature which is depicted in the term global warming‘ (Stocker *et al*., 2013). For most of the world, the instrumental measurements of temperature started in the 19th Century or later (Brohan *et al*., 2006).

Tree ring cellulose is one of the primary sources of information about climatic variability reaching beyond the industrial revolution (Mann & Jones, 2003; Mann *et al*., 2008; Brienen *et al*., 2012). Global climate models use these reconstructions to test the behaviours of various processes in the past (Ahmed *et al*., 2013). Tree ring data is preferred for modelling studies because they have the most stable resolution, i.e. its resolution does not change with the age of the sample. Using statistical techniques, the reconstructed climate variability from tree ring width shows a 40-50% variance with the instrumentally observed data (Borgaonkar *et al*., 2011). Isotopic techniques provide better measurement precision, as Sharp (2017) explained in his book Principle of Stable Isotope Geochemistry. The effective precision of a stable isotope measurement is much higher than that is immediately apparent from the stated precision of a δ value, which in the best case is ± 0.01‰. For example, the $\delta^{18}O$ value of + 2.05‰ corresponds to an absolute ratio of 0.002009311, while that of + 2.06‰ is 0.002009331. So, a difference of 0.01‰ translates to a change in the eighth decimal place. Using a calibration equation, the isotopic ratio analysis provides better precision. However, statistical climate-tree ring analysis yields similar levels of explained variance for tree-ring width and stable isotope proxies. E.g. Liu *et al.*, 2014 explained 43% of the variance of May-July mean temperatures, and Treydte *et al*. (2009) were able to reproduce ~ 60% of the climate variance using non-linear statistical methods.

Due to climate zones ranging from subtropical to glacial and forests varying between temperate to alpine, the western Himalayas are rich with tree ring data sets covering Kinnaur in Himachal Pradesh, Kothi-Kanasar in Uttarakhand, and eastern Nepal (e.g. Borgaonkar *et al*., 1999; Yadav *et al*., 2011; Sano *et al*., 2017; Yadava *et al*., 2021). Most tree-ring studies discuss humidity, precipitation, or drought variation (e.g. Sano *et al*., 2017; Yadava *et al*., 2021). By using ring-width data from a site in Uttarakhand, Yadava *et al*. (2021) reconstructed June-July-August Palmer Drought Severity Index (JJAPDSI) with variance varying from 0.43 to 0.406. Sano *et al*. (2017) used tree-ring oxygen isotope data from Manali, Himachal Pradesh, to reconstruct June–September Self-Calibrated (sc) PDSI with a variable variance of 38.5 to 55.8%. Yadav and Singh (2002) reconstructed ~400 years of spring temperature patterns with ~50% variance. Tree ring inferred summer temperature variations over the past millennium from Lahaul-Spiti was reconstructed by Yadav *et al.* (2011) with ~58% explained variance. Tree-ring oxygen isotope variations in subalpine Firs of Magguchatti Valley, Himachal Pradesh capture spring temperature signals (Chinthala *et al*., 2022) with a maximum variance of 30%. Tree ring oxygen isotope northern slope of the western Himalayas also showed similar variance with temperature (Huang *et al*., 2019).

The physiochemical process of cellulose formation and the isotopic fractionation can be modelled by experimentation on live trees (Farquhar *et al*., 1982; Roden *et al*., 2000; Hughes, 2002). Several groups have been working on modelling tree biochemical processes to establish relations between meteorological parameters like relative humidity and soil moisture with isotopic compositions of tree ring cellulose (Roden *et al*., 2000; McCarroll & Loader, 2004). These relations have been used as forward models to calculate isotopic values of wood cellulose (Evans, 2007). The ensemble means of these constructions which produce the best fit with observed isotopic values using correlations and pattern recognition techniques were taken as meteorological parameters in the period of cellulose formation (Managave *et al*., 2010). Treydte *et al*., 2009 calculated in long-term data plant physiological response to increasing atmospheric CO_2 concentration. Bose *et al*. 2014 quantified the effect with respect to temperature and humidity. Bose *et al.* (2016) reconstructed soil water oxygen isotope values from tree ring cellulose data of thirteen stations around the globe using a process-based reverse reconstruction model (Equation I).

Tree-ring width and isotope values are a complex function of air temperature, humidity, soil moisture, soil nutrients, and species level effects. The statistical analysis tries to separate these dependencies which is usually not possible in these extremely non-linear systems. The present research does not assume that the tree ring cellulose oxygen isotope as proxy for any particular parameter but tests how to extract temperature information from the complex non-linear function using a numerical solution. The present work modifies the model used in Bose *et al*. (2016) to reconstruct air temperature from tree ring cellulose oxygen isotope values using oxygen isotope data of *Picea smithiana* samples from Kothi, Himachal Pradesh, India generated by us. This reconstruction does not require any calibration and hence can be directly compared to instrumental data.

MODEL

The reconstruction of the soil water oxygen isotopic composition (δ_{sw}) as outlined in equation 4 of Bose *et al*. (2016) is given below:

$$\delta_{sw} = \frac{\delta_c - N_0}{D_0} \quad \text{(I)}$$

where:

$$N_0 = C_{11} + N_1 + \delta_{ah} N_2 \quad \text{(Ia)}$$

$$C_{11} = f_O \epsilon_{OH} + (1 - f_O)\epsilon_{OA} - 1000(1 - f_O)(1 - p_v) \quad \text{(Ib)}$$

p_v = advected un-enriched water in the leaf

$$N_1 = 1000\alpha_L^*(1 - f_O)(1 - p_v)\left\{\alpha_k \frac{e_l - e_{ls}}{e_l} + \alpha_{kb}\frac{e_{ls} - e_a}{e_l} + \frac{e_a}{e_l}\right\} \quad \text{(Ic)}$$

e_l = Leaf vapour pressure (kPa)

e_{ls} = Leaf surface vapour pressure (kPa)

e_a = atmospheric vapour pressure (kPa)

$$N_2 = \alpha_L^*(1 - f_O)(1 - p_v)\frac{e_a}{e_l} \quad \text{(Id)}$$

$$D_0 = f_O + (1 - f_O)p_v + \alpha_L^*(1 - f_O)(1 - p_v)\left\{\alpha_k \frac{e_l - e_{ls}}{e_l} + \alpha_{kb}\frac{e_{ls} - e_a}{e_l}\right\} \quad \text{(Ie)}$$

We simplified equation I as above with δ_{sw} as known leading to the following equation. It is to be noted that the terms T_1, K_1, x_1, K_2, x_2, T_2, etc. are used here to simplify the representation of the equation and do not have any physical significance unless otherwise mentioned.

Residual, $R = T_1 - (K_1 x_1 + K_2 x_2 + T_2) = 0$ (1)

Where,

$$T_1 = 2PC_s \frac{\delta_c - f_O \epsilon_{OH} + (1-f_O)(\epsilon_{OA} - 1000) - f_O \delta_{sw}}{1 - f_O} \tag{1.1}$$

$$K_1 = \delta_{sw} - 1000 \tag{1.2}$$

$$x_1 = (C_A - C_1 g) R_{hf} x + \alpha_L^* \{C_B + C_C y\} + (C_D + 2PC_s) R_{hf} z + (1 - \alpha_{kb}) R_{hf}^2 z^2 \} \tag{1.3}$$

$$C_A = C_1 \alpha_k g \tag{1.3.1}$$

$$C_1 = 101.325 \tag{1.3.1.1}$$

$$C_B = 2P\{\alpha_{kb} C_s + (\alpha_k - \alpha_{kb}) g\} \tag{1.3.2}$$

$$C_C = C_1(-2\alpha_k + \alpha_{kb}) g \tag{1.3.3}$$

$$C_D = \alpha_k + 2P\{(-1)\alpha_k + \alpha_{kb}\} g - 2P\alpha_{kb} C_s \tag{1.3.4}$$

$$x = exp\ exp\ (T_{Ea}) \tag{1.3.5}$$

$$T_{Ea} = -0.1299 T_{aK}^{-4} + 1.1641 T_{aK}^{-3} - 4.6889 T_{aK}^{-2} - 6.9134 T_{aK}^{-1} + 10.5681 \tag{1.3.5.1}$$

$$T_{aK} = \frac{\{273.16 + T_a\ (yr)\}}{373.16} \tag{1.3.5.1.1}$$

$$y = exp\ exp\ (T_{EL}) \tag{1.3.6}$$

$$T_{EL} = -0.1299 T_{LK}^{-4} + 1.1641 T_{LK}^{-3} - 4.6889 T_{LK}^{-2} - 6.9134 T_{LK}^{-1} + 10.5681 \tag{1.3.6.1}$$

$$T_{LK} = T_{aK} - d_{Tr} \tag{1.3.6.1.1}$$

$$d_{Tr} = \Delta T / 373.16 \tag{1.3.6.1.1.1}$$

$$z = \frac{x}{y} \tag{1.3.7}$$

$$K_2 = \frac{\delta_c - f_O \epsilon_{OH} + (1-f_O)(\epsilon_{OA} - 1000) - f_O \delta_{sw}}{1 - f_O} \tag{1.4}$$

$$x_2 = C_1 g y - R_{hf} z \tag{1.5}$$

$$T_2 = D_{RO} \alpha_L^* R_{hf} (2PC_s \frac{x}{y} - C_1 g x + R_{hf}) z^2 \tag{1.6}$$

$$D_{RO} = \frac{1.137 \times 10^6}{(273.16 + T_a)^2} - \frac{0.4156 \times 10^3}{273.16 + T_a} - 2.0667 \tag{1.6.1}$$

DATA USED

To validate the transformed model (equation Eq. (1)), we used various datasets as detailed below:

Isotope data

We analyzed *Picea smithiana* samples from montane sites with 2850 to 3000 m altitude above mean sea level around Kothi, Himachal Pradesh, India (KOHP) from those dendrochronologically dated by Borgaonkar *et al.* (2011) from a montane site at a steep incline. A part of the carbon isotope ($\delta^{13}C$) data from the same set of samples has already been reported by Bose *et al.* (2014). Bose *et al.* (2016) used part of the oxygen isotope dataset carbon and oxygen isotope data are reported in ‰ VPDB and VSMOW, respectively.

Additionally, we have used tree ring oxygen isotope datasets from twelve stations across the globe (Ballantyne *et *al*., 2011; Managave *et al*., 2011; Kress *et al*., 2010; Treydte *et al*., 2009; Holzkämper *et al*., 2008; Saurer *et al*., 2008). These were the same oxygen isotope datasets used in Bose *et al.* (2016).

To calculate Δ_{cC}, atmospheric $\delta^{13}C$ of atmospheric CO_2 (1977−2008 CE) data from 11 Scripps Institution of Oceanography stations were used in the present study (Keeling *et al*., 2005). We used a simple quadratic fit (global $\delta^{13}C_a$ as a function of time; r = 0.99) to estimate the global annual average of $\delta^{13}C_a$ before 1977. We assumed that $\delta^{13}C_a$ was -6.40‰ before human activities changed it (McCarroll *et al*., 2009). This method is similar to Bose *et al*. (2014).

Meteorological data

T_a, e (CRU-3.10) and R_{hf} (CRU-3.10.01) data was taken from the CRU dataset (Harris *et al.*, 2013; Mitchell & Jones, 2005). This monthly average dataset with a 0.5°× 0.5° spatial resolution: (i) has the highest resolution, (ii) is available at all the site locations for a longer time duration (1901-2008 CE) compared to other similar datasets. R_{hf} is computed from the existing T_a and e using the formula:

$$R_{hf} = \frac{e}{e_{sat}} \qquad (4)$$

where:

e_{sat} = saturation vapour pressure of water

$$= 1.33\, exp\left(20.386 - \frac{5132}{273.16 + T_a}\right) \qquad (4.1)$$

Equation 4 is the best fit curve obtained by regressing the temperature data with the e_{sat} (Murphy & Koop, 2005) according to the analytical method outlined in List (1963) for the normal temperature range.

Atmospheric pressure (P) data averaged over a long period (1979-2004) was taken from ERA-interim (Dee *et al*., 2011) for the respective tree sites to be used in equation 3.1, etc. This data set has very small variability for P (maximum 2.4%) for these sites hence the average value is used for all years.

RESULTS AND DISCUSSION

From comparing source water reconstructions for all sites in Bose *et al.* (2016), we have found that the following equation is correct with the coefficient of determination (R^2) above 0.8 (Table 1):

$$\delta_{sw} = m_O\delta_c + i_O \qquad (2)$$

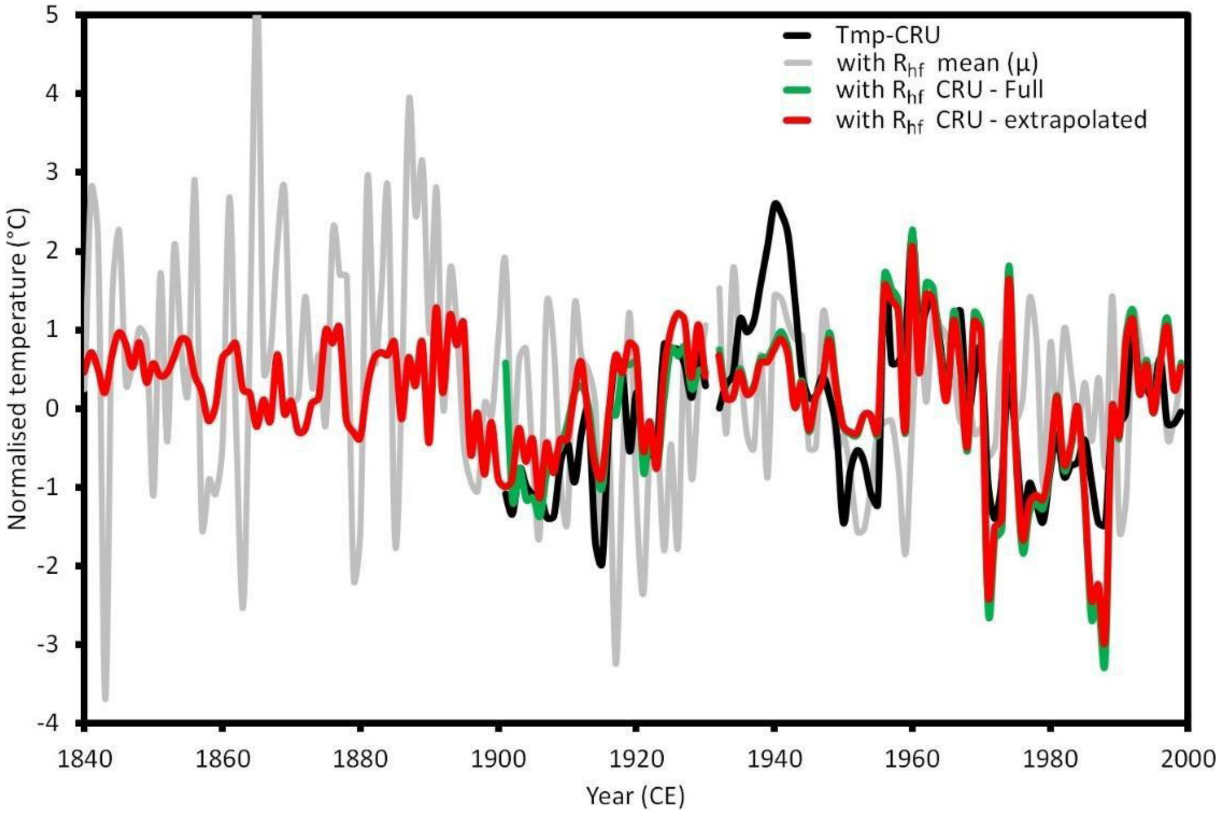

Fig. 1—Reconstructed temperature with the input of (i) mean (1901-1999 CE) R_{hf} (light Grey), (ii) R_{hf} (1901-1999 CE) from CRU (Green), and (iii) extrapolated R_{hf} (Red) in comparison with CRU temperature (Black) for the site KOHP.

Table 1—Slope, intercept and r^2 value of δ_{swO} vs. δ_{cO} lines for all sites given with respect to their latitude.

	Latitude	Slope	Intercept	r^2
MRR1	68	1.02	-39.83	0.98
MRR2	68	1.00	-40.80	0.97
VISW	48	1.00	-40.95	0.99
LOSW	46	1.00	-39.01	0.97
CASW	46	1.04	-40.71	0.95
BOIB	37	0.99	-36.79	0.97
BAGR	36	0.99	-38.17	0.97
KOHP	32	1.00	-37.96	0.98
J2CH	19	1.04	-32.69	0.91
J1CH	19	1.05	-31.79	0.86
PAKE	10	1.16	-35.22	0.90
PMPE	-13	0.97	-27.62	0.80
VGPE	-22	0.95	-32.80	0.93

Eq. (1) cannot be solved analytically, hence, a numerical solution is required. Prof. V. K. Gaur (personal communication) suggested to calculate the Residual, R for all possible values of δ_{cO} against those of T_a (i values) and R_{hf} (j values). Then the minima of $|R| = \sqrt{(R_{i,j} - R_{min})^2}$ with respect to a particular δ_{cO} leads to the correct values of T_a and R_{hf}. This method is dependent on Eq. (1) having a single minimum with respect to δ_c. The value of R_{min} was calculated for T_a = -200 to 200 C, R_{hf} = 0.00 to 0.99, and δ_{cO} = -10 to 40‰ to test this postulation. In this test, the range of T_a needed to be increased significantly to find the minimum point of R due to dramatic changes in the range of parameters in the non-linear model. This increase in the T_a range is only a mathematical assumption to adjust for non-linearity. It is to be noted that R depends on both T_a and R_{hf}, hence we need to provide one to reconstruct the other. Further, the distribution of R has to be calculated for each time step and |R| needs to be minimized among various testing temperatures to estimate the correct temperature. Due to the increased range of T_a, the reconstructed temperature is compared with the observations in the normalized form. The normalization has been done with respect to the average value of each series for 1901-1999 CE.

The model was tested for:

1. mean R_{hf} for all years
2. R_{hf} (1901-1999 CE) from CRU
3. extrapolated R_{hf} for the period before meteorological data was available (Fig. 1). We extrapolated by the Burg method using autoregressive power spectral density (Stern *et al.*, 2002) which is quite accurate in small range extrapolation with a calibration period of 90 years (in the testing period of 9 years, r = 0.91, p <0.01)
4. Carbon isotope discrimination (Δ_{cC}) of tree ring cellulose of the same sample set is the most available option as R_{hf} proxy with the same time duration and resolution. Δ_{cC} is a complex function of humidity and temperature via leaf evapouration along with pCO_2 of air which has been used as a proxy for humidity in several articles (e.g., Fonti *et al.*, 2021; Liu *et al.*, 2018). In the western Himalayas, Bose *et al.*, 2014 quantified the effect of relative humidity on carbon isotope in the 20th Century but did not reconstruct humidity before 1900 CE. To use in the model, Δ_{cC} was linearly mapped to the range of R_{hf} for each site, leading to a matching amplitude but not in phase.

The oxygen and hydrogen isotope pathways for cellulose are the same which means that Eq. (1) can be written for hydrogen in a similar form. Hence, if hydrogen data of the same set of samples are available, both can be minimized to give simultaneous reconstructions of both temperature and relative humidity. Hence, hydrogen isotope data of the same samples would be the best option for this situation but there is no such dataset available to test the combined model.

For case (1) the phase information of the CRU data and the reconstruction mostly match but the amplitude is not in accordance (Fig. 1). The cases (2) and (3) gave correlations of 0.73 and 0.75 respectively (p <0.0001) for the same period with a good phase and amplitude match. A comparison of the reconstructed temperature with CRU data in the observed period shows that the reconstructed temperature has no lag with the instrumental data even when average R_{hf} is used for all years. The temperature shows larger inter-annual variability after 1970 compared to pre-1970 years. The only visible problem is in the case (3) reconstruction showing a continuously increasing temperature trend going back from 1901 which is inconsistent compared to other reconstructions of this period. Hence, another proxy for R_{hf} is required for reconstructions.

These reconstructions (Fig. 1) do not have any calibration or testing periods as they have not been calibrated against any observed temperatures. The reconstruction is not site-specific, as shown by the similar results from site BOIB using data from (Treydte *et al.*, 2009) for case (2). This case also has a correlation of 0.72 (p <0.0001) with the observed data (Fig. 2) and shows the climate change effect after 1970 CE. Both reconstructions show some incoherency with the CRU temperatures from the respective sites which may be understood by the fact that CRU data from this region are generated from very sparse observational networks.

The KOHP site reconstruction for case (4) (Fig. 3) shows that apart from a few reverse peaks, e.g. ~1984, 1958 CE, the temperature trends and amplitudes are well reproduced. The main problem visible in this reconstruction stems from the

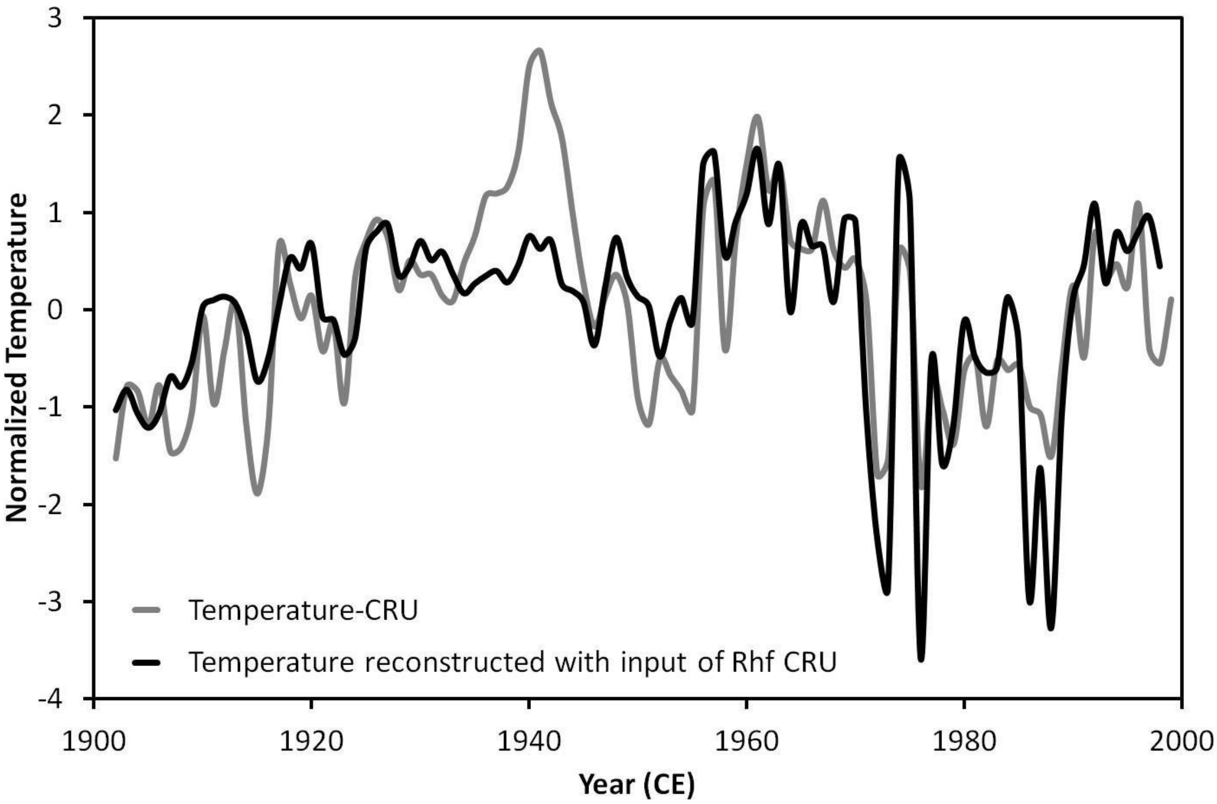

Fig. 2—Reconstructed temperature with the input of R_{hf} (1901-1999 CE) from CRU (black) compared with CRU temperature (grey) for the site BOIB.

observation that Δ_{cC} data seems to add additional frequency components to the reconstruction. In the pre-1935 years, the peaks and troughs mostly match though values are slightly different. Possible causes behind these observations are:

A. The Δ_{cC} variability depends on Ta and R_{hf} (Bose *et al.*, 2014) and inserting it directly as R_{hf} leads to a circular calculations adding many additional phases to the reconstruction.
B. The differences in CRU and reconstruction might be due to modelling problems in the generation of CRU data without instrumental validation for this isolated area. This problem is seen in case (1) during 1935-65 indicating that in this period, the model does not reproduce the CRU values even with R_{hf} calculated using CRU data. It is to be noted that this is the period of second world war followed by aerial nuclear explosions which stopped with the Nuclear Test-Ban Treaty of 1963, which banned above ground nuclear weapons testing. Possible cause behind this effect might be that upper tropospheric heating might be affecting the temperature humidity relationship at high altitudes.
C. The problems mentioned in A and B separately or in combination are leading to more variation during 1955-2000 for case 4 possibly in relation to Climate Change.

CONCLUSIONS AND IMPLICATIONS

The above analysis indicates that the model as presented provides consistent site- independent temperature reconstruction without the requirement of any calibration. The main requirement for long-term temperature reconstruction using this model is corresponding R_{hf} data or a proxy for the same.

It should be noted that as the pathways of oxygen and hydrogen isotopes in cellulose are the same, a similar equation can be established for hydrogen. Hence, if hydrogen data of the same set of samples are available, both can be minimized to give simultaneous reconstructions of both temperature and relative humidity.

Acknowledgements—*Authors thank Dr. M. Saurer, PSI, Switzerland and all others who have contributed their data to the NOAA paleoclimate database. Prof. V.K. Gaur provided invaluable ideas for mathematical analysis. Guidance from Late Prof. R. Ramesh is earnestly acknowledged. Dr. Vandana Prasad and Prof. M.G. Thakkar, the former and current Directors of Birbal Sahni Institute of Palaeosciences, Lucknow, India are sincerely recognized for sustained motivation (BSIP/RDCC/01/22-23). Prof. B.N. Goswami, Dr. M.N. Rajeevan, Prof. Ravi Shankar Nanjundiah and*

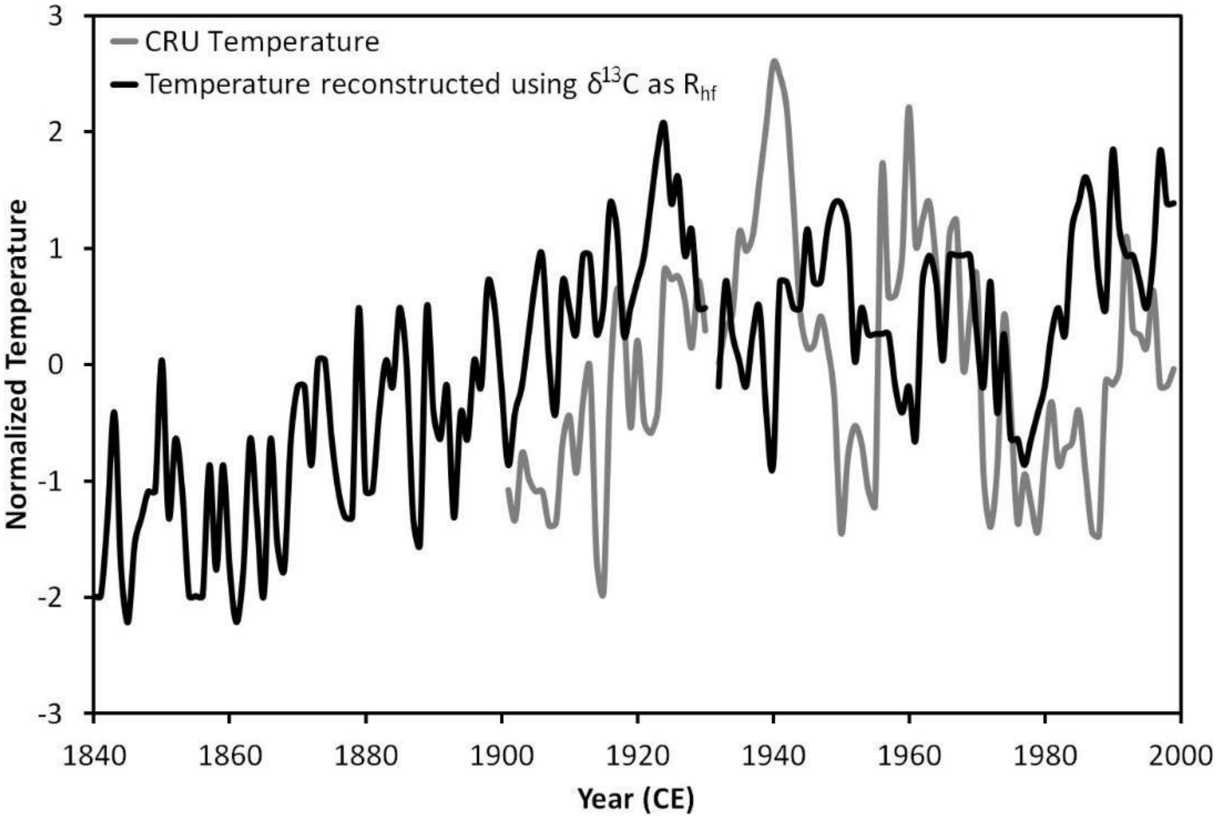

Fig. 3—Reconstructed temperature using Δ_{cC} as input values. This was mapped to the range of R_{hf} (1901-1999 CE) in black compared with CRU temperature (Gray) for the site KOHP.

Dr. R. Krishnan, the former and current Directors of the Indian Institute of Tropical Meteorology, Pune, India were source of constant encouragement. The authors special gratitude goes to the reviewers of this manuscript for their invaluable corrections leading to significant improvement to the article.

REFERENCES

Ahmed M, Anchukaitis K, Buckley BM, Braida M, Borgaonkar HP, Asrat A, Cook ER, Büntgen U, Chase BM, Christie DA *et al*. 2013. Continental-scale temperature variability during the past two millennia: Supplementary information. Nature Geoscience 6(5): 339-346.

Ballantyne A, Baker P, Chambers J, Villalba R & Argollo J 2011. Regional differences in south American monsoon precipitation inferred from the growth and isotopic composition of tropical trees. Earth Interactions 15(5): 1-35.

Barnosky AD 2014. Palaeontological evidence for defining the Anthropocene. Geological Society London Special Publications 395(1): 149-165.

Borgaonkar HP, Pant GB & Kumar KR 1999. Tree-ring chronologies from western Himalaya and their dendroclimatic potential. IAWA journal 20(3): 295-309.

Borgaonkar H, Sikder A & Ram S 2011. High altitude forest sensitivity to the recent warming: A tree-ring analysis of conifers from western Himalaya, India. Quaternary International 236(1): 158-166.

Bose T, Chakraborty S, Borgaonkar H, Sengupta S & Ramesh R 2014. Estimation of past atmospheric carbon dioxide levels using tree-ring cellulose $\delta^{13}C$. Current Science 107(6): 971-982.

Bose T, Sengupta S, Chakraborty S & Borgaonkar H 2016. Reconstruction of soil water oxygen isotope values from tree ring cellulose and its implications for paleoclimate studies. Quaternary International 425: 387-398.

Brienen RJ, Helle G, Pons TL, Guyot JL & Gloor M 2012. Oxygen isotopes in tree rings are a good proxy for amazon precipitation and El Niño-Southern Oscillation variability. Proceedings of the National Academy of Sciences 109(42): 16957-16962.

Brohan P, Kennedy JJ, Harris I, Tett SF & Jones PD 2006. Uncertainty estimates in regional and global observed temperature changes: A new data set from 1850. Journal of Geophysical Research: Atmospheres 111(D12).

Cappa CD, Hendricks MB, DePaolo DJ & Cohen RC 2003. Isotopic fractionation of water during evapouration. Journal of Geophysical Research: Atmospheres 108(D16).

Chinthala BD, Grießinger J, Ranhotra PS, Tomar N, Singh C & Bräuning A 2022. Tree-ring oxygen isotope variations in subalpine firs from the western Himalaya capture spring season temperature signals. Forests 13(3): 437.

Dee D, Uppala S, Simmons A, Berrisford P, Poli P, Kobayashi S, Andrae U, Balmaseda M, Balsamo G, Bauer P *et al.* 2011. The era-interim reanalysis: Configuration and performance of the data assimilation system. Quarterly Journal of the Royal Meteorological Society 137(656): 553-597.

Evans M 2007. Toward forward modeling for paleoclimatic proxy signal calibration: A case study with oxygen isotopic composition of tropical woods. Geochemistry, Geophysics, Geosystems 8(7).

Farquhar GD, O'Leary M & Berry J 1982. On the relationship between carbon isotope discrimination and the intercellular carbon dioxide concentration in leaves. Functional Plant Biology 9(2): 121-137.

Fonti M, Siegwolf R, Kirdyanov A, Knorre A, Trushkina T, Myglan V, Vaganov E, Saurer M *et al*. 2021. Response of temperature-limited forests to recent moisture changes derived from tree-ring stable carbon isotopes. Russian Journal of Ecology 52(5): 368-375.

Harris I, Jones P, Osborn T & Lister D 2013. Updated high-resolution grids of monthly climatic observations - the CRU TS3.10 dataset. International Journal of Climatology URL: http://dx.doi.org/10.1002/joc.3711

Holzkämper S, Kuhry P, Kultti S, Gunnarson B & Sonninen E 2008. Stable isotopes in tree rings as proxies for winter precipitation changes in the Russian Arctic over the past 150 years. Geochronometria 32(1): 37-46.

Huang R, Zhu H, Liang E, Grießinger J, Wernicke J, Yu W, Hochreuther P, Risi C, Zeng Y, Fremme A & Sodemann H 2019. Temperature signals in tree-ring oxygen isotope series from the northern slope of the Himalaya. Earth and Planetary Science Letters 506: 455-465.

Hughes MK 2002. Dendrochronology in climatology-the state of the art. Dendrochronologia 20(1): 95-116.

Keeling CD, Piper SC, Bacastow RB, Wahlen M, Whorf TP, Heimann M & Meijer HA 2005. Atmospheric CO_2 and $^{13}CO_2$ exchange with the terrestrial biosphere and oceans from 1978 to 2000: observations and carbon cycle implications. *In*: Baldwin IT, Caldwell MM, Heldmaier G, Jackson RB, Lange OL, Mooney HA, Schulze ED, Sommer U, Ehleringer JR, Dearing MD *et al*. (Editors)-A history of atmospheric CO_2 and its effects on plants, animals, and ecosystems. Springer: 83-113.

Kress A, Saurer M, Siegwolf RT, Frank DC, Esper J & Bugmann H 2010. A 350-year drought reconstruction from alpine tree ring stable isotopes. Global Biogeochemical Cycles 24(2).

Lewis SL & Maslin MA 2015. Defining the Anthropocene. Nature 519(7542): 171-180.

List RJ 1963. Smithsonian meteorological tables. Smithsonian Institution.

Liu Y, Wang Y, Li Q, Song H, Linderholm, HW, Leavitt SW, Wang R & An Z 2014. Tree-ring stable carbon isotope-based May–July temperature reconstruction over Nanwutai, China, for the past century and its record of 20th Century warming. Quaternary Science Reviews 93: 67-76.

Liu Y, Ta W, Li Q, Song H, Sun C, Cai Q, Liu H, Wang L, Hu, S, Sun J *et al*. 2018. Tree-ring stable carbon isotope-based April June relative humidity reconstruction since AD 1648 in Mt. Tianmu, China. Climate Dynamics 50(5): 1733-1745.

Majoube M 1971. Fractionation of oxygen-18 and of deuterium between water and its vapour. Journal Chimie Physique 68: 1423-1436.

Managave S, Sheshshayee M, Borgaonkar H & Ramesh R 2010. Past break-monsoon conditions detectable by high resolution intra-annual $\delta^{18}O$ analysis of teak rings. Geophysical Research Letters 37(5).

Managave S, Sheshshayee M, Ramesh R, Borgaonkar H, Shah S & Bhattacharyya A 2011. Response of cellulose oxygen isotope values of teak trees in differing monsoon environments to monsoon rainfall. Dendrochronologia 29(2): 89-97.

Mann ME & Jones PD 2003. Global surface temperatures over the past two millennia. Geophysical Research Letters 30(15).

Mann ME, Zhang Z, Hughes MK, Bradley RS, Miller SK, Rutherford S & Ni F 2008. Proxy-based reconstructions of hemispheric and global surface temperature variations over the past two millennia. Proceedings of the National Academy of Sciences 105(36): 13252-13257.

McCarroll D, Gagen MH, Loader NJ, Robertson I, Anchukaitis KJ, Los S, Young GH, Jalkanen R, Kirchhefer A & Waterhouse JS 2009. Correction of tree ring stable carbon isotope chronologies for changes in the carbon dioxide content of the atmosphere. Geochimica et Cosmochimica Acta 73(6): 1539-1547.

McCarroll D & Loader NJ 2004. Stable isotopes in tree rings. Quaternary Science Reviews 23(7): 771-801.

Mitchell TD & Jones PD 2005. An improved method of constructing a database of monthly climate observations and associated high-resolution grids. International Journal of Climatology 25(6): 693-712.

Murphy D & Koop T 2005. Review of the vapour pressures of ice and supercooled water for atmospheric applications. Quarterly Journal of the Royal Meteorological Society 131(608): 1539-156.

Roden JS, Lin G & Ehleringer JR 2000. A mechanistic model for interpretation of hydrogen and oxygen isotope ratios in tree-ring cellulose. Geochimica et Cosmochimica Acta 64(1): 21-35.

Sano M, Dimri A, Ramesh R, Xu C, Li Z & Nakatsuka T 2017. Moisture source signals preserved in a 242-year tree-ring $\delta^{18}O$ chronology in the western Himalaya. Global and Planetary Change 157: 73-82.

Saurer M, Cherubini P, Reynolds-Henne C, Treydte K, Anderson W & Siegwolf R 2008. An investigation of the common signal in tree ring stable isotope chronologies at temperate sites. Journal of Geophysical Research 113(G4): G04035.

Sharp Z 2017. Principles of Stable Isotope Geochemistry, 2nd Edition. doi: https://doi.org/10.25844/h9q1-0p82.

Steffen W, Leinfelder R, Zalasiewicz J, Waters CN, Williams M, Summerhayes C, Barnosky AD, Cearreta A, Crutzen P, Edgeworth M *et al*. 2016. Stratigraphic and earth system approaches to defining the Anthropocene. Earth‘s Future 4(8): 324-345.

Stern AS, Li KB & Hoch JC 2002. Modern spectrum analysis in multidimensional NMR spectroscopy: comparison of linear-prediction extrapolation and maximum-entropy reconstruction. Journal of the American Chemical Society 124(9): 1982-1993.

Stocker T, Qin D, Plattner GK, Tignor M, Allen S, Boschung J, Nauels A, Xia Y, Bex V & Midgley P, eds 2013. IPCC 2013: Summary for policymakers. Cambridge University Press.

Treydte KS, Frank DC, Saurer M, Helle G, Schleser GH & Esper J 2009. Impact of climate and CO_2 on a millennium-long tree-ring carbon isotope record. Geochimica et Cosmochimica Acta 73(16): 4635-4647.

Yadav RR & Singh J 2002. Tree-ring-based spring temperature patterns over the past four centuries in western Himalaya. Quaternary Research 57(3): 299-305.

Yadav RR, Braeuning A & Singh J 2011. Tree ring inferred summer temperature variations over the last millennium in western Himalaya, India. Climate Dynamics 36(7): 1545-1554.

Yadava AK, Misra KG, Singh V, Misra S, Sharma YK & Kotlia BS 2021. 244-year-long tree-ring-based drought records from Uttarakhand western Himalaya, India. Quaternary International 599: 128-137.